iScience

CellPress
OPEN ACCESS

Article

Chronic carbon disulfide exposure induces parkinsonian pathology via α-synuclein aggregation and necrosome complex interaction

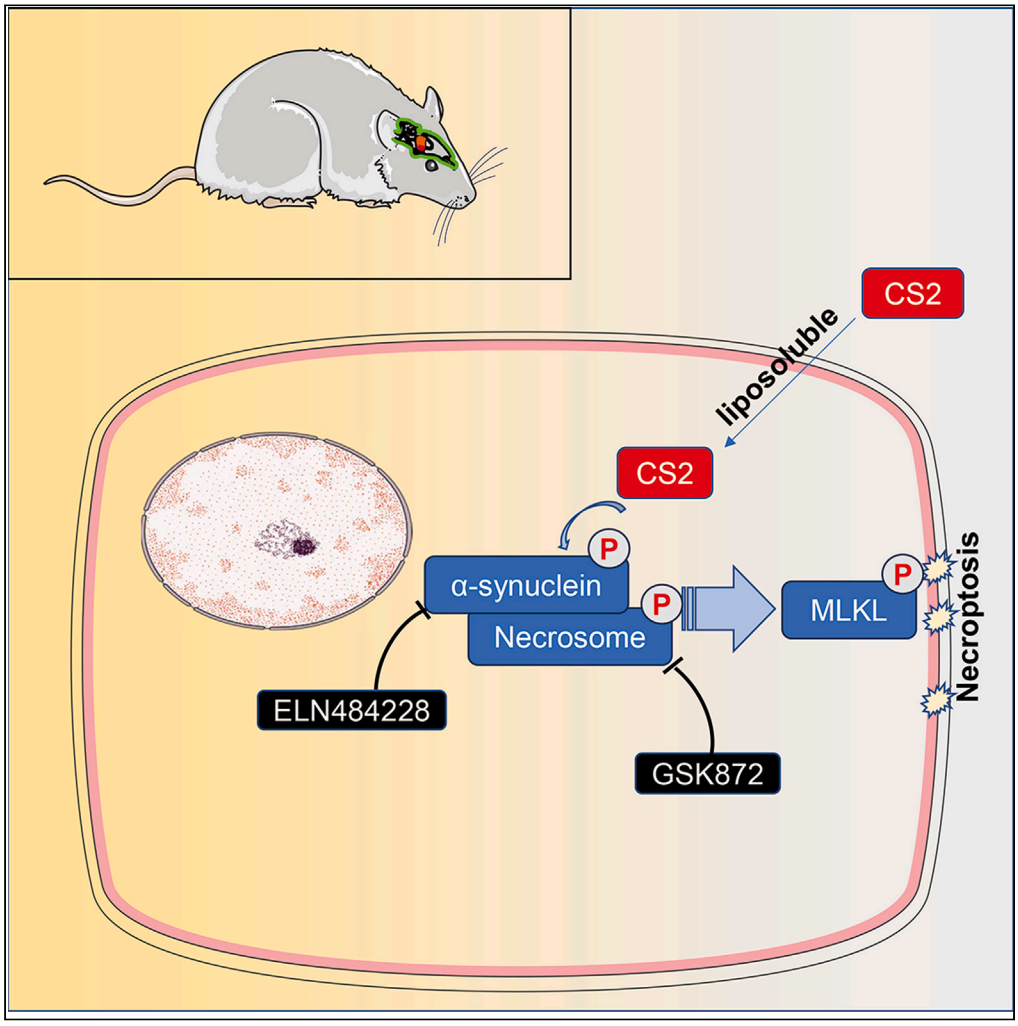

Zhidan Liu, Kang Kang, Shulin Shan, ..., Yanan Sun, Yao Bai, Fuyong Song

baiyao@cfsa.net.cn (Y.B.)
fysong3707@sdu.edu.cn (F.S.)

Highlights

Carbon disulfide induces α-synuclein aggregation and phosphorylation in neurons

Carbon disulfide induces necroptotic signaling pathway activation in neurons

Carbon disulfide promotes α-synuclein interacts with necrosome complex

α-synuclein inhibition alleviates carbon disulfide-induced necroptosis

Liu et al., iScience *26*, 107787
October 20, 2023
https://doi.org/10.1016/j.isci.2023.107787

iScience

CellPress
OPEN ACCESS

Article

Chronic carbon disulfide exposure induces parkinsonian pathology via α-synuclein aggregation and necrosome complex interaction

Zhidan Liu,[1] Kang Kang,[2] Shulin Shan,[1] Shuai Wang,[1] Xianjie Li,[3] Hui Yong,[2] Zhengcheng Huang,[1] Yiyu Yang,[1] Zhaoxiong Liu,[1] Yanan Sun,[1,4] Yao Bai,[4,*] and Fuyong Song[1,5,*]

SUMMARY

Exposure to carbon disulfide (CS_2) has been associated with an increased incidence of parkinsonism in workers, but the mechanism underlying this association remains unclear. Using a rat model, we investigated the effects of chronic CS_2 exposure on parkinsonian pathology. Our results showed that CS_2 exposure leads to significant motor impairment and neuronal damage, including loss of dopaminergic neurons and degeneration of the substantia nigra pars compacta (SNpc). The immunoassays revealed that exposure to CS_2 induces aggregation of α-synuclein and phosphorylated α-synuclein, as well as activation of necroptosis in the SNpc. Furthermore, *in vitro* and *in vivo* experiments demonstrated that the interaction between α-synuclein and the necrosome complex (RIP1, RIP3, and MLKL) is responsible for the loss of neuronal cells after CS_2 exposure. Taken together, our results demonstrate that CS_2-mediated α-synuclein aggregation can induce dopaminergic neuron damage and parkinsonian behavior through interaction with the necrosome complex.

INTRODUCTION

Parkinson's disease (PD) is one of the most common neurodegenerative diseases,[1] which is characterized by early prominent loss of dopaminergic neurons (DNs) in the substantia nigra and the presence of Lewy bodies (LBs).[2] Although the etiology of PD remains enigmatic, genetics, environment, and interactions are generally thought to be relevant.[2] An empirical analysis suggests the greater the social growth in gross national income, the faster the incidence of Parkinson's disease rises,[3] reinforcing the neurological dangers of environmental pollution. MPTP was the first environmental toxin reported to induce a PD-like syndrome in humans after exposure,[4] to date, other environmental toxins that have been convincingly associated with PD include the pesticide rotenone, the herbicide paraquat, the fungicide maneb,[5] and the solvent trichloroethylene (TCE).[6,7] Carbon disulfide (CS_2) is a listed environmental contaminant, and its neurotoxicity was observed in rubber workers as early as 1856.[8] Case reports and cross-sectional studies found that viscose rayon manufacturers with decades of CS_2 exposure had an increased incidence of parkinsonism.[9–11] CS_2-derived dithiocarbamates (DTCs), which are widely used in fungicides and insecticides, are associated with PD by inducing severe CNS depression.[12–14] One study also found that environmental toxicants, including DTC, can promote the development of PD.[15] Nevertheless, the molecular mechanisms of the association between CS_2 exposure and PD remain unclear.

Necroptosis is a form of regulated necrotic cell death that is mediated by necrosome complex (consist by receptor-interacting protein kinase 1 (RIPK1 or RIP1), RIP3, and mixed lineage kinase domain-like protein (MLKL)).[16] In the mature nervous system, necroptosis is the primary cell death enforcer in response to extracellular inflammatory signals, particularly in the setting of apoptosis deficiency.[17] In recent years, many evidences suggest that necroptosis is associated with dopaminergic neuronal death in PD. For example, one study showed that inhibiting RIP1 by necrostatin-1 ameliorated neuronal loss in MPTP-treated mice, a classic toxin-treated PD model.[18] In addition, knockdown of the RIP3/MLKL gene blocked the necrotic pathway and greatly improved PD by increasing dopamine levels and rescuing the loss of dopaminergic neurons, independent of the apoptotic pathway.[19] Aggregates of α-synuclein form the core of LBs and are therefore considered to be the main pathogenic protein of PD.[20] In a recent study, selumetinib reduced acrolein-induced α-synuclein aggregation, RIP1/RIP3 protein expression and protected cell survival,[21] similar results occurred in gallic acid-blocked lipopolysaccharide (LPS)-induced injury.[22] However, whether α-synuclein can cause necroptosis has not yet been reported.

CS_2 has widespread CNS toxicity, the pathological anatomy showed cerebral atrophy, basal ganglia and especially striatum damage in human postmortem.[23,24] Experiments of rat exposure to CS_2 also observed primary neuronal degeneration. For example, CS_2-induced

[1]Department of Toxicology and Nutrition, School of Public Health, Cheeloo College of Medicine, Shandong University, Jinan, Shandong 250012, China
[2]Qingdao Municipal Center for Disease Control & Prevention, Qingdao, Shandong 266033, China
[3]Institute of Biological and Medical Engineering, Guangdong Academy of Sciences, Guangzhou, Guangdong 510075, China
[4]NHC Key Laboratory of Food Safety Risk Assessment, China National Center for Food Safety Risk Assessment, Beijing 100021, China
[5]Lead contact
*Correspondence: baiyao@cfsa.net.cn (Y.B.), fysong3707@sdu.edu.cn (F.S.)
https://doi.org/10.1016/j.isci.2023.107787

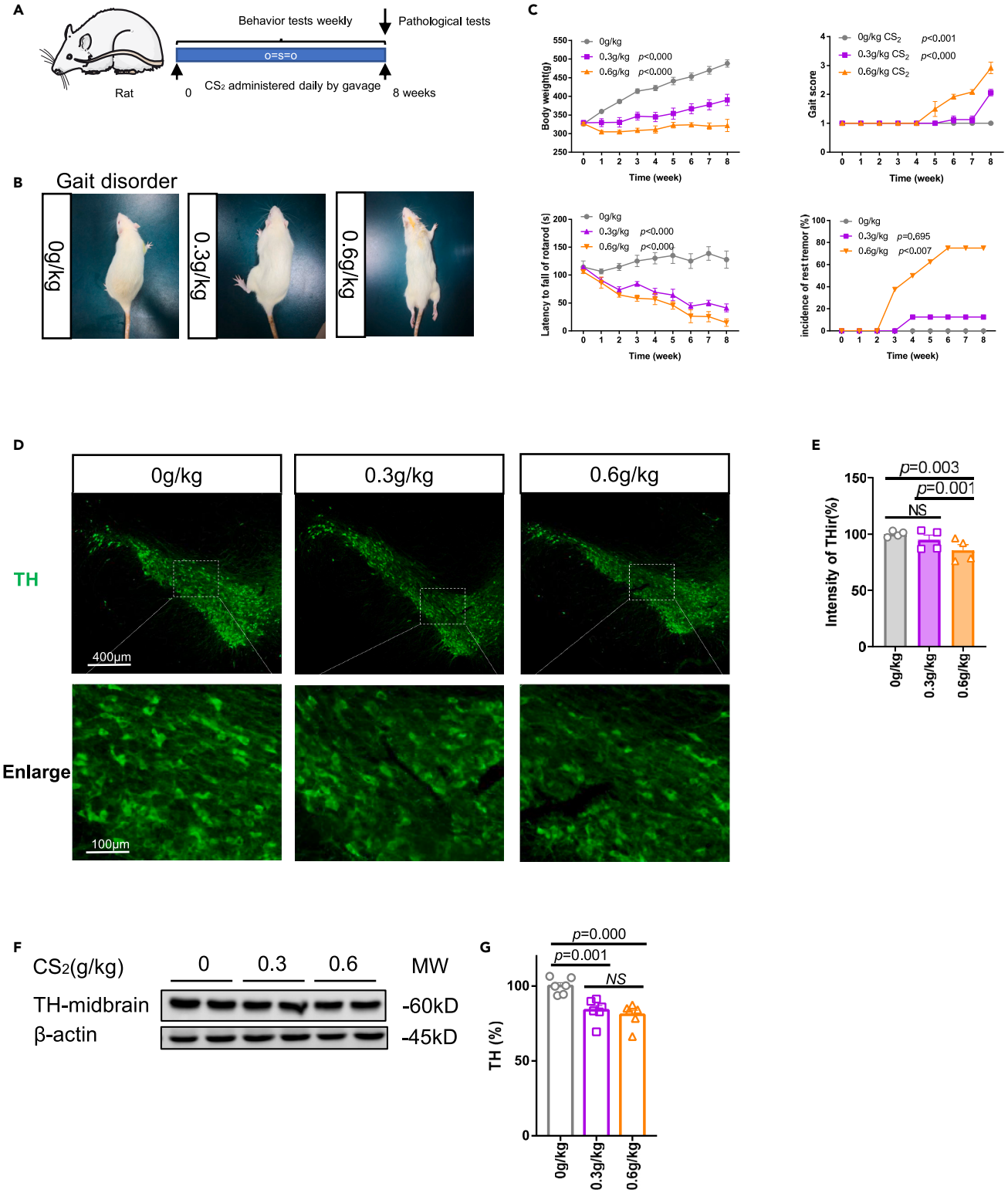

Figure 1. CS_2-exposed rats display motor impairment and dopaminergic neurons degeneration

(A) Experimental design for CS_2 exposure in Westar rats.

(B) Performance of behavior after 8 weeks of administration of CS_2.

Figure 1. *Continued*

(C) Behavior assessment of male rats following CS_2 treatment for 8 weeks. CS_2-treated rats showed defects on the body weight test, the latency to fall of rotarod test, the gait point assessment, and the incidence of resting tremor assessment.

(D and E) Frozen sections of rat brains containing SNpc were stained with anti-TH antibodies (D). Fluorescence intensity of TH staining was counted (E).

(F and G) The midbrain protein of the rat was extracted and immunoblotted with an anti-TH antibody (F), and TH protein levels were quantified (G). (C), (E), and (G) show means ± SEM, p value is comparison with control group by t test.

morphologic lesions of the brain related to the cerebral cortical, cerebellum, midbrain, and brain stem appeared after several weeks of treatment,[25] characterized by cytoplasm shrunken or swollen, axon degeneration, neurofilaments aggregation, and ATP content reduction,[26,27] neurons of hippocampus subregions CA1 and CA3 declined significantly by immune staining.[28,29] As a linear, non-polar molecule with high lipophilicity,[30,31] CS_2 can also freely cross the blood-brain barrier (BBB) and biological membranes. CS_2 can react directly with biological molecules in the brain of mammals, including nucleophilic addition of amines, sulfhydryls, and hydroxyls to reversibly yield DTCs, trithiocarbonates (TTCs), and xanthates, respectively. In addition, DTCs can generate isothiocyanate and subsequently form covalent protein cross-links. The proteins b-lactoglobulin, porcine neurofilaments, bovine serum albumin, and hemoglobin were each observed to react with CS_2 to form thiourea-based cross-links and dimers; lysine E-amines were predominantly involved.[32] Whether CS_2 and its metabolites can promote α-synuclein aggregation through protein cross-linking mechanisms to induce neuronal cell loss is well worth investigating.

To address the underlying mechanism connecting CS_2 exposure to parkinsonism, a rat model of chronic CS_2 exposure through intragastric administration was established. Our findings support the hypothesis that CS_2 exposure leads to significant motor impairment and neuronal damage. Furthermore, exposure to CS_2 induces α-synuclein aggregation and phosphorylation, as well as activation of necroptosis pathways in the SNpc. Specifically, *in vitro* and *in vivo* experiments demonstrated that the interaction between α-synuclein and the necrosome complex is responsible for the loss of neuronal cells after CS_2 exposure. This study provides insight into the pathological mechanism underlying CS_2-induced parkinsonism and highlights the importance of further investigating the necrosome complex in PD.

RESULTS

Motor deficits and dopaminergic neuron injury in CS_2 exposed rats

To investigate the clinical and pathological performance of CS_2 exposure in rats, we first selected male Wistar rats to create a dose-gradient exposure model (Figure 1A). According to the exposure dose, the rats were divided into a control group (0 g/kg BW), a low-dose CS2 exposure group (0.3 g/kg BW), and a high-dose CS2 exposure group (0.6 g/kg BW). To evaluate the motor deficits after CS_2 exposure, behavioral experiments were performed weekly for 8 weeks (Figures 1B and 1C). We found that the body weight growth and the latency to fall of rotarod were significantly lower in the CS_2 exposure group rats than in the control. The gait score was also significantly higher in the CS_2 exposure group rats than in the control. The resting tremor in the low-dose group and high-dose group rats first emerged in week 4 and week 3, respectively, and the incidence increased to 12.5% and 75.0% in week 8, respectively, compared with the control group rats remained at 0%. These results indicate that CS_2 exposure induces motor dysfunction.

Given the significant motor deficits observed in CS_2-exposed rats, whether dopaminergic neurons in the SNpc were damaged after CS_2 exposure was investigated. We first examined dopaminergic neurons in the frozen section using antibodies specific to tyrosine hydroxylase (TH) which is a dopamine rate-limiting enzyme. (Figure 1D). Quantification of TH-positive staining indicates active dopaminergic neurons within the SNpc. We found that CS_2-exposed rats showed a significant decrease in TH staining compared to the control. (Figure 1E). TH protein expression in the midbrain was also measured (Figure 1F), and the protein level of TH in CS_2-exposed rats showed a significant decrease (Figure 1G) compared to the control. These results indicate that CS_2 exposure decreased dopaminergic neuron activity in SNpc.

CS_2 exposure induces synaptic injury

Synaptic and mitochondrial injuries are hallmarks of dopaminergic neuron damage. First, we examined synaptophysin (SYN) expression in frozen sections (Figure 2A). We conducted SYN and TH co-staining to investigate the synaptic integrity of dopaminergic neurons within the SNpc, a significantly decreased co-staining in CS_2-exposed rats was observed compared to the control group (Figures 2B and 2C). Next, transmission electron microscopy (TEM) was performed on fixed sections of the SNpc (Figure 2D). The average areas of dendrites, synapses, and mitochondria in them were counted after CS_2 exposure (Figure 2E). Compared with the control group, the area of mitochondria in dendritic (Mito in Den), axon terminal (At), and axon terminal per dendritic (At by Den) was significantly reduced, respectively, in CS_2-exposed rats. These results indicate that CS_2 exposure damages dopaminergic neuron synapses.

Necroptosis of dopaminergic neurons was activated after CS_2 exposure

The damage to dopaminergic neurons after CS_2 exposure was demonstrated previously, and we further explored the mechanism of cell loss. For this purpose, we first detected the necroptosis signaling in the midbrain (Figure 3A), the protein level of RIP1, p-RIP1, RIP3, p-RIP3, MLKL, and *p*-MLKL in the CS_2-exposed groups; all showed a significant increase compared with the control (Figure 3B). Meanwhile, we examined necroptosis in SNpc using a frozen section with anti-*p*-MLKL and anti-TH antibodies; we labeled *p*-MLKL and TH to investigate the necroptosis of dopaminergic neurons within the SNpc (Figure 3C). CS_2-exposed groups showed a significant increase than the control (Figures 3D and 3E). *In Situ* Cell Death Detection and TEM were also performed in SNpc (Figures 3F and 3G), this indicates the cell death of dopaminergic neurons after CS_2 exposure.

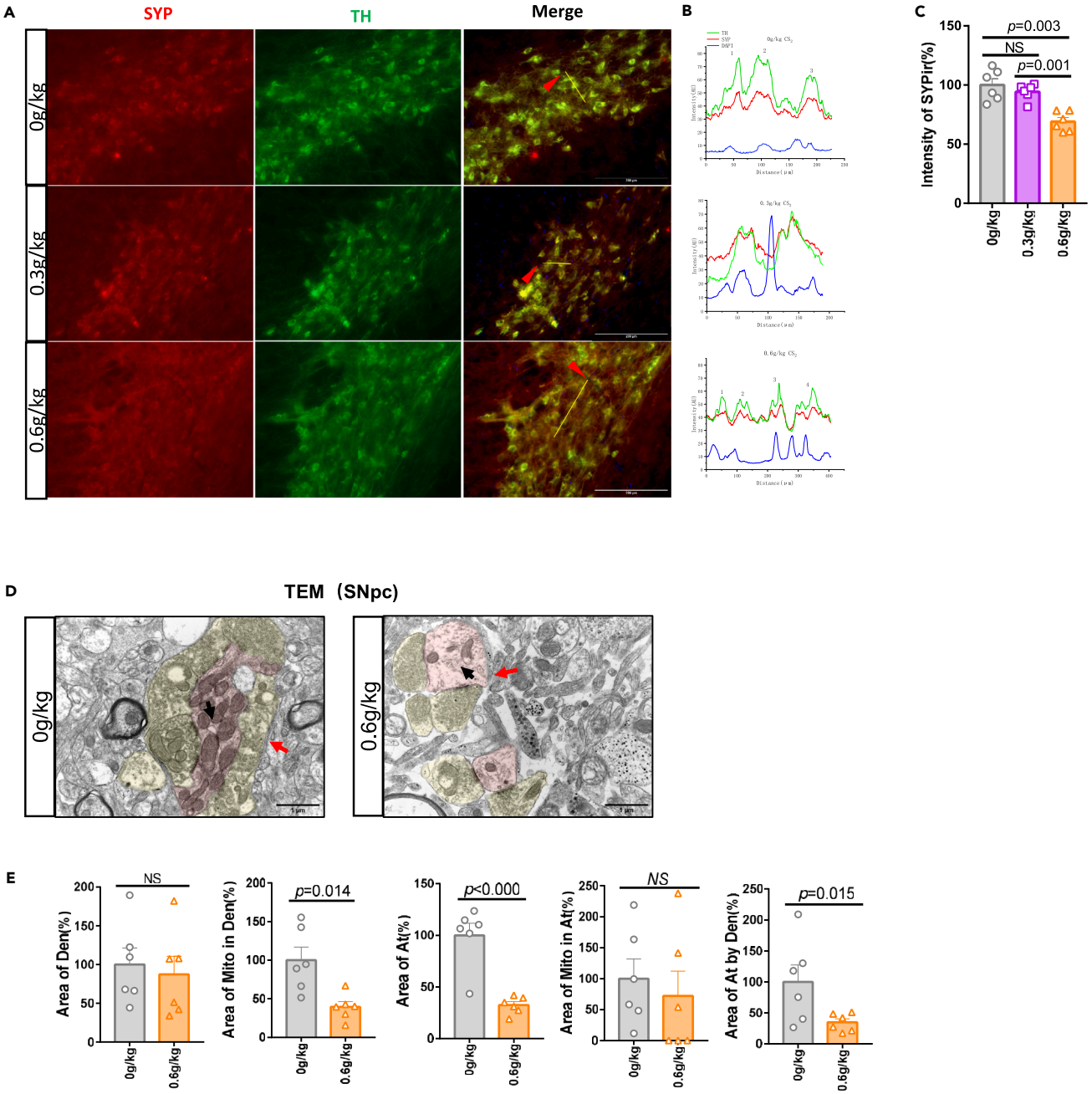

Figure 2. CS_2 leads to synaptic injury

(A–C) Frozen sections of rat brains containing SNpc were co-stained with anti-SYP antibodies and anti-TH antibodies and observed by fluorescence microscope (A). The yellow line represents the location of the line analysis (B), and the intensity of SYP staining was counted (C).

(D and E) Transmission electron microscopy (TEM) was performed on fixed sections of rat brains containing SNpc (D). The average areas of dendrites (Den), axon terminals (At), and their mitochondria were counted (E). (C), (E) show means ± SEM, p value is comparison with control group by t test.

RIP3 blocking protects the activation of necroptotic signaling in SH-SY5Y cells

To further verify the key role of necroptotic signaling pathway in the loss of dopaminergic neurons, RIP3 inhibitor GSK872 (antagonizing necroptosis) was utilized to intervene in SH-SY5Y cell lines subjected to CS_2 (Figure 4A). The necroptotic signaling activating after dose-sequence CS_2 exposure on SH-SY5Y cells was first examined (Figure 4B), and our results showed that the protein level of *p*-MLKL, the killer protein of necroptosis in CS_2-exposed groups showed a significant increase compared with the control (Figure 4C). Next, the necroptotic signaling activating after RIP3-blocker GSK872 against CS_2 treatment was tested (Figure 4D); *p*-MLKL protein in GSK872 pre-administration group showed

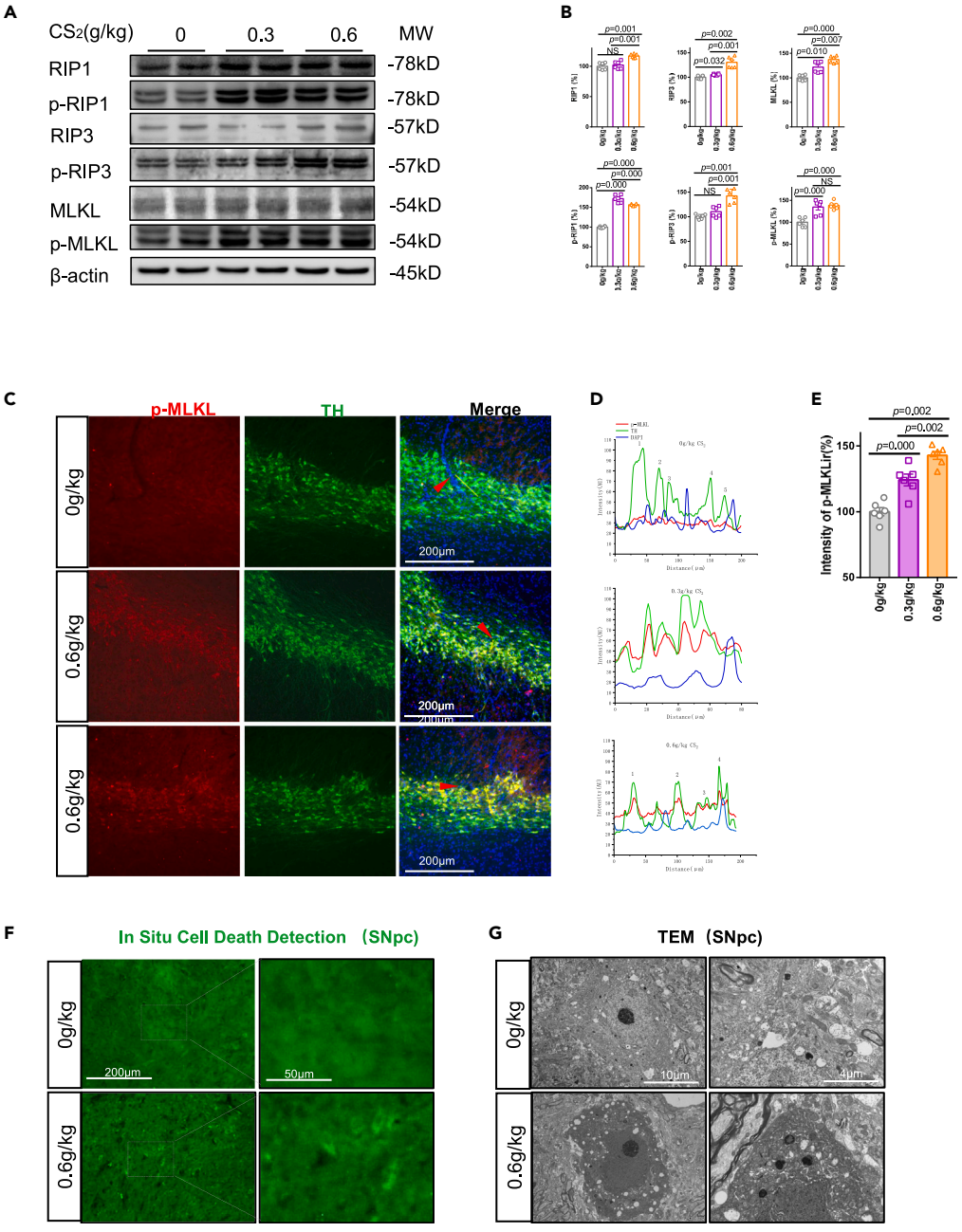

Figure 3. CS_2 activation necroptosis signaling in dopaminergic neurons

(A and B) The midbrain protein was extracted and immunoblotted with anti-RIP1, anti-p-RIP1, anti-RIP3, anti-p-RIP3, anti-MLKL, and anti-*p*-MLKL antibody (A), and the proteins level was quantified (B).

(C–E) Frozen sections of rat brains containing SNpc were co-stained with anti-*p*-MLKL and anti-TH antibodies (C). The yellow line represents the location of the line analysis (D), and the Intensity of *p*-MLKL staining was counted (E).

(F) Frozen sections of rat brains containing SNpc were stained with *In Situ* Cell Detection Kit and observed by fluorescence microscope.

(G) Transmission electron microscopy (TEM) was performed on fixed sections of rat brains containing SNpc. (B) and (E) show means ± SEM, p value is comparison with control group by *t test*.

an attenuated expression than CS_2-exposed group (Figure 4E). The same results were obtained in the GSK872 on cells treated with different doses of CS_2 (Figures S1A and S1B). The optical microscope picture also showed that cell loss was attenuated by GSK872 (Figures 4F and 4G). These results indicate that GSK872 effectively attenuated CS_2 induced necroptosis.

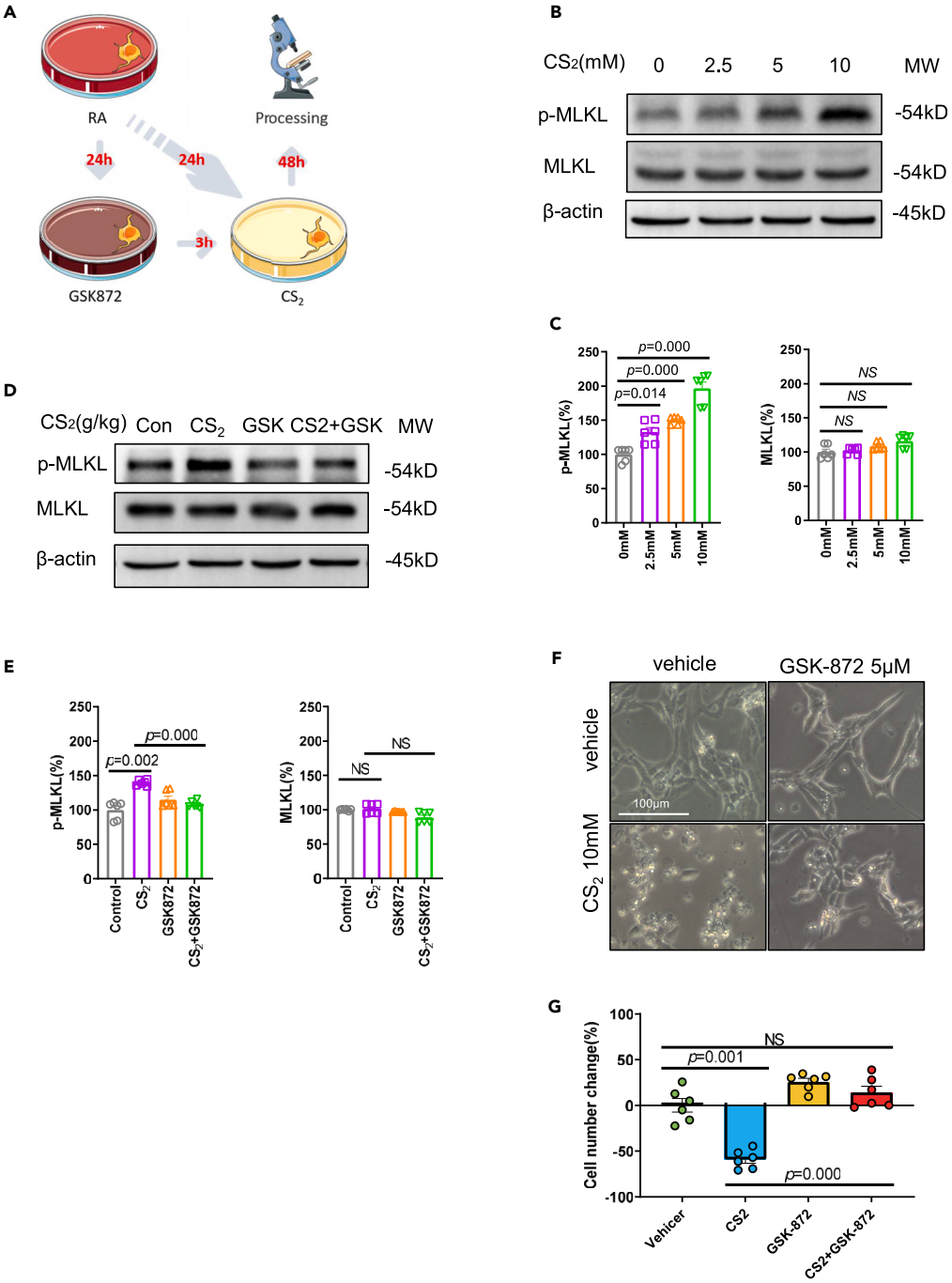

Figure 4. CS_2 induced necroptotic signaling activating and cell loss was attenuated by GSK872

(A) SH-SY5Y cells was cultured and exposed to dose-sequence CS_2 or exposed to 10mM CS_2 which pre-intervention with 5μM GSK872.

(B and C) Protein of SH-SY5Y cells that dose-sequence CS_2 exposed was extracted and immunoblotted with anti-MLKL, and anti-*p*-MLKL antibody (B), and the proteins level was quantified (C).

(D and E) Protein of SH-SY5Y cells that GSK872 interferes was extracted and immunoblotted with anti-MLKL and anti-*p*-MLKL antibody (D), and the proteins level was quantified (E).

(F and G) SH-SY5Y cells after GSK872 intervention were pictured using a light microscope (F) and counted (G). (C), (E), and (G) show means ± SEM, p value is comparison with control group by t test.

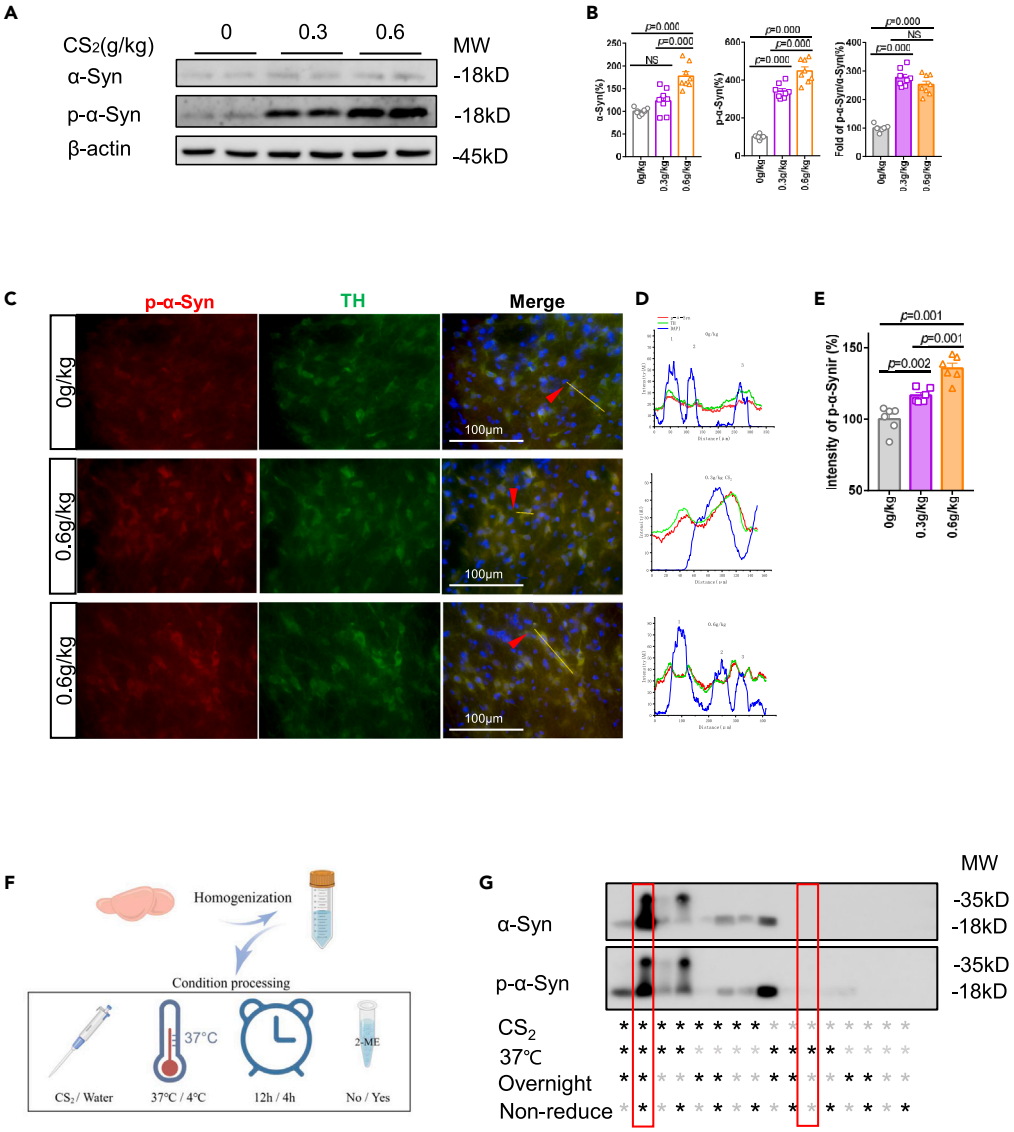

Figure 5. CS_2 induces α-synuclein aggregation and phosphorylation in dopaminergic neurons

(A and B) The midbrain protein of the rat was extracted and immunoblotted with anti-α-synuclein (anti-α-Syn) and anti-phosphorylated α-synuclein (anti-p-α-Syn) antibodies (A), and the protein level was quantified (B).

(C–E) Frozen sections of rat brains containing SNpc were co-stained with anti-p-α-Syn and anti-TH antibodies (C). The yellow line represents the location of the line analysis (D), and the intensity of p-α-synuclein staining was counted (E).

(F and G) The midbrain protein of untreated rat was co-incubated with CS_2 in an *in vitro* environment (F), and immunoblotted with anti-αS and anti-p-α-Syn, antibodies (G), black dot * means exposure to CS_2 in a 37°C, overnight environment and non-reducing loading buffer processing, pale dot * means the contrast. (B) and (E) show means ± SEM, p value is comparison with control group by t test.

CS_2 induced aberrant accumulation of α-synuclein and phosphorylated α-synuclein in the dopaminergic neuron

As α-synuclein was believed to be closely related to dopaminergic neuron damage in Parkinson's disease, we investigated whether CS_2 influences the accumulation of α-synuclein and phosphorylated α-synuclein in dopaminergic neurons. To this end, protein expression of α-synuclein and α-synuclein phosphorylated in serine 129 (p-α-synuclein) in the midbrain was first measured (Figure 5A), the protein level of α-synuclein and p-α-synuclein in CS_2-exposed rats showed a significant increase compared with the control (Figure 5B). Next, we further examined p-α-synuclein expression in frozen sections (Figure 5C). Quantification of p-α-synuclein and TH co-staining, indicative of the α-synuclein phosphorylation within a dopaminergic neuron, showed a significant increase in CS_2-exposed rats compared with the control (Figures 5D and 5E). Because CS_2 can react directly crosslink with some proteins in mammals to form adducts,[33] we conducted an *in vitro* reaction system to further determine whether CS_2 can directly induce α-synuclein aggregation and phosphorylation (Figure 5F); the protein

expression level of α-synuclein and phosphor-α-synuclein was measured and significantly increased in CS_2-exposed groups than in the control at 37°C, overnight, and non-reduced environmental conditions (Figure 5G). Our data indicate that exposure to CS_2 enhanced the aberrant accumulation of α-synuclein and phosphorylation of α-synuclein in rats.

α-synuclein blocking protects the phosphorylation of α-synuclein and activation of necroptotic signaling in SH-SY5Y cells

To reinforce the impact of α-synuclein on the necroptosis signaling pathway, the α-synuclein inhibitor ELN484228 was utilized to intervene in SH-SY5Y cell lines subjected to CS_2 (Figure 6A). The phosphorylation of α-synuclein after dose-sequence CS_2 exposure on SH-SY5Y cells was first examined (Figure 6B); the protein level of α-synuclein, p-α-synuclein in CS_2-exposed groups showed a significant increase compared with control (Figure 6C). Next, α-synuclein blocker ELN484228 was tested on SH-SY5Y cells prior to CS_2 treatment (Figure 6D). Our results showed an attenuated α-synuclein, p-α-synuclein protein expression in ELN484228 pre-administration group than CS_2-exposed group, and the protein expression of *p*-MLKL was hypoactive simultaneously after ELN484228 pre-administration (Figure 6E). The optical microscope results also showed an attenuated cell loss by ELN484228 (Figures 6F and 6G). In order to determine the specificity of ELN484228's inhibitory effect on α-synuclein after CS_2 exposure, we continued to detect the protein expression of α-synuclein and p-α-synuclein after GSK872 intervention, and the protein expression of α-synuclein and p-α-synuclein showed unchanging in GSK872 pre-administration group than the CS_2-exposed group (Figures S2A and S2B). These results indicate that ELN484228 effectively attenuated necroptosis and cell loss and strengthened the link between α-synuclein and necrosome.

α-synuclein interacts with necrosome *in vivo* in the rat brain, *in vitro*, and in silico

Based on the aforementioned results, α-synuclein aggregation and necroptosis signal activation occurring simultaneously, we predict that CS_2-induced damage to dopamine neurons may be caused by affecting α-synuclein accumulation, and α-synuclein may directly activate the necroptosis signal. To confirm our point, we first tested whether α-synuclein interacts with necroptosis signal-related proteins in the midbrain of exposed rat by co-immunoprecipitation (Figure 7A). We found that α-synuclein can directly interact with RIP1, RIP3, and MLKL, and the extent was significantly increased after exposure to CS_2. Further, these interactions are related to CS_2 exposure in rat and SH-SY5Y cells (Figures 7B and 7C), the SH-SY5Y cell line, which can express TH protein and mimics human dopaminergic neurons *in vitro*. These results indicate that α-synuclein can interact with necrosome, and this interaction was promoted by CS_2 exposure. Next, we investigate the interaction between α-synuclein and necrosome at the atomic level (Table 1), three different forms of α-synuclein protein (PDB:6i42, PDB:3q25, PDB:1xq8), and necrosome proteins include RIP1 (PDB:4itj), RIP3 (PDB:7mx3), MLKL (PDB:4mwi), and RIP3-MLKL complex (PDB:7mon) were obtained from protein databank (PDB), and computational analysis was performed in PDBePISA. In these results, α-synuclein interacts strongly with RIP3 and RIP3-MLKL complex (Figures 7D and 7E). These results have established a strong link between the α-synuclein protein and the necrosome complex.

DISCUSSION

PD caused by environmental factors has attracted attention. As an industrial solvent, CS_2 causes severe damage to the nervous system, and the association between CS_2 and PD has been observed from the earliest pathological reports, but this association lacks experimental verification. Herein, we establish a rat model subchronically exposed to CS_2. In our results, CS_2-exposed rats show motor deficits including rest tremor and progressive paralysis. Rest tremor first appeared in the 3rd week, and its incidence increased to 80% of the rats in the 6th week after CS_2 exposure. For rotenone, rest tremor occurred in only 25% of all treated 16 mice, usually by day 30.[34] Rest tremor occurring in the rat has not been reported. In early experimental studies, eight dogs exposed to CS_2 fumes also exhibited symptoms of extrapyramidal lesions.[35] The injuries we observed in animal models corresponded to case reports of workers, many of whom have signs of PD such as rest tremor and bradykinesia after decades of exposure to CS_2.[36] For example, a patient who had worked in a viscose rayon factory and was exposed to high concentrations of carbon disulfide for 46 years till he notices impaired short recall memory, mental slowness, depressive feelings, and signs of Parkinsonism with rigidity and tremor mainly of the upper extremities at the age of 59 years. Although he soon had to stop working, the symptoms were gradually progressive.[37]

Early neuronal cell death is one of the major pathological hallmarks of neurodegenerative diseases; several primary regions of the brain suffer neuronal loss.[38] A clinical study found that on average, at least 50% of nigral neurons were lost before the neurologist could make a positive diagnosis of a patient with PD.[39] After long-term exposure to CS_2, patients disclosed mild cortical atrophy, and multiple lesions in the subcortical white matter and basal ganglia by CT and MRI. Brain CT angiography and perfusion also revealed a significant decrease of cerebral blood flow and a decrease of cerebral blood volume in the basal ganglia. In our results, dopaminergic neurons in SNpc showed a significant loss and were accompanied by SNpc areas shrinking in rats' brains after CS_2 exposure. Dendrite and axon terminal damage accompanied by loss of mitochondria in the SNpc was also shown after CS_2 exposure. This emphasizes the role of reduced innervations of neurons, except exacerbating cell death.[38] It has long been suggested that apoptosis is the chosen pathway for eliminating dopaminergic neurons. However, in this work, regarding the protein level of caspase-3 and cleaved caspase-3, an apoptosis executive protein, there was no significant change detected. Necroptosis is another form of programmed cell death involved in degenerative diseases.[40] Necroptosis is mediated by a signaling complex containing RIP1, RIP3, and MLKL. The latest study found that it is the RIP1-RIP3 interaction that empowers to recruit of other free RIPK3; homodimerization of RIPK3 triggers its autophosphorylation and thus can recruit MLKL to execute necroptosis.[41] There has been a claim that necroptosis may be also involved in the death pathways of PD, an *in vivo* study showed that Nec-1, a potent

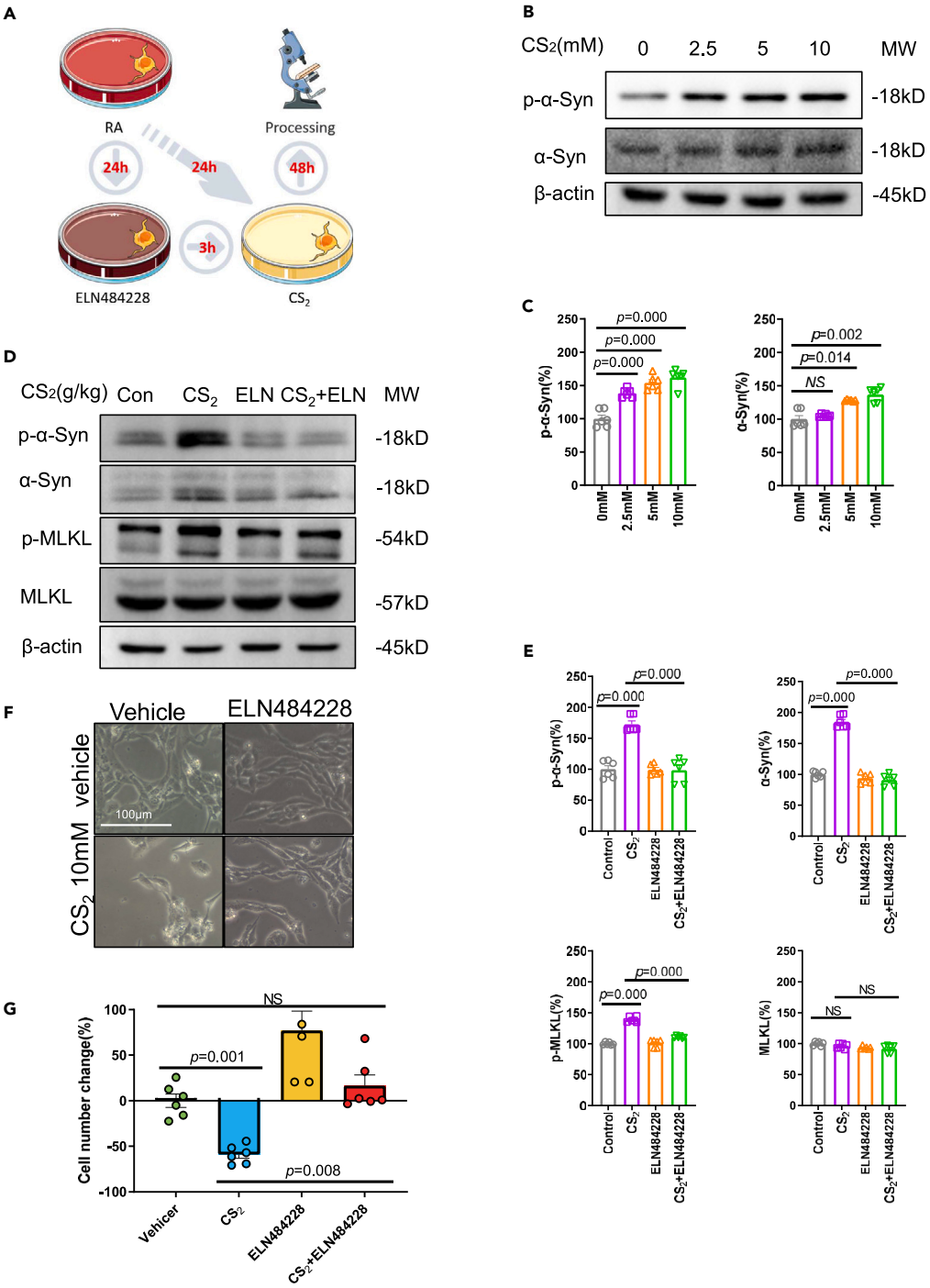

Figure 6. CS_2-induced α-synuclein aggregation/phosphorylation and necroptotic signaling activating was attenuated by ELN484228

(A) SH-SY5Y cells was cultured and exposed to dose-sequence CS_2 or exposed to 10mM CS_2 which pre-intervention with 5μM ELN484228.

(B and C) Protein of SH-SY5Y cells that dose-sequence CS_2 exposed was extracted and immunoblotted with anti-MLKL, and anti-*p*-MLKL antibody (B), and the proteins level was quantified (C).

(D and E) Protein of SH-SY5Y cells that ELN484228 interferes was extracted and immunoblotted with anti-MLKL, and anti-*p*-MLKL antibody (D), and the proteins level was quantified (E).

(F and G) SH-SY5Y cells after ELN484228 intervention were pictured using a light microscope (F) and counted (G). (C), (E), and (G) show means ± SEM, p value is comparison with control group by *t test*.

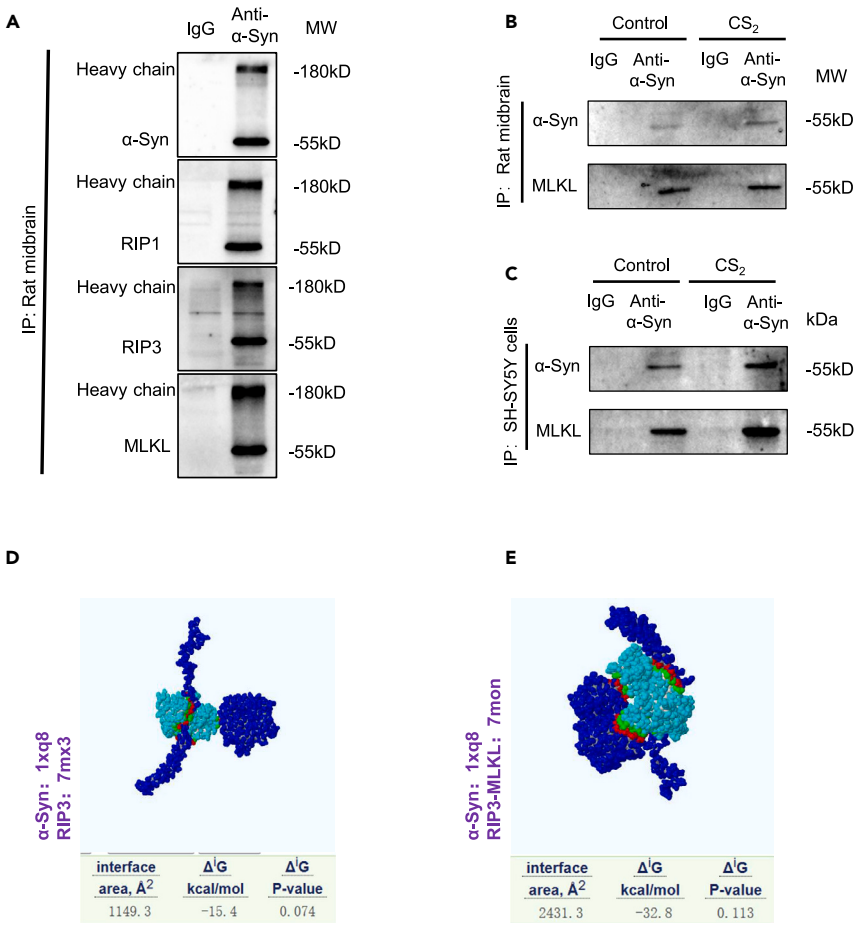

Figure 7. Aggregated α-synuclein interacts with RIP3-MLKL complex *in vitro*, *in vivo*, and in silico

(A) The midbrain protein of the rat was extracted and co-immunoprecipitation with anti-α-Syn antibody and rabbit IgG respectively, then, immunoblotted with anti-α-Syn and anti-RIP1, anti-RIP3 and anti-MLKL antibody.

(B) The midbrain protein of the rat was extracted and co-immunoprecipitation with anti-α-Syn antibody and rabbit IgG respectively, then, immunoblotted with anti-α-Syn and anti-MLKL antibody.

(C) Total cell lysate protein of SH-SY5Y cells was extracted and co-immunoprecipitation with anti-α-Syn antibody and rabbit IgG, respectively, then, immunoblotted with anti-α-Syn and anti-MLKL antibody.

(D) α-Syn protein (1xq8) and RIP3 protein (7mx3) were obtained from PDB and interactive simulations using PDBePISA.

(E) α-Syn protein (1xq8) and RIP3-MLKL complex (7mon) were obtained from PDB and interactive simulations using PDBePISA.

inhibitor of RIP1, ameliorated neuronal loss in MPTP-treated mice.[42] Interestingly, our work showed that necroptotic signaling was activated in DNs in SNpc in rats. Meanwhile, we used human-derived SH-SY5Y cells, which are capable of expressing TH proteins, to mimic dopaminergic neurons exposure to CS_2 *in vitro*, also showed an activated necroptotic signaling. In sum, the loss of dopaminergic neurons after CS_2 exposure was mainly attributed to necroptosis, while, how necroptotic signaling was activated needs further studies.

The presence of LBs which mainly consists of α-synuclein and ubiquitin[43] is another typical pathological manifestation of PD. The discovery of mutations in the gene for α-synuclein (SNCA) in familial PD solidified the etiologic importance of α-synuclein to PD.[43] α-Synuclein has the propensity to misfold, become insoluble, and form β-sheet-rich amyloid aggregates that accumulate and form intracellular inclusions; the intermediates including oligomeric and proto-fibrillar are toxic forms that can finally cause neuronal degeneration.[44] Direct misfolding of α-synuclein into pathogenic conformers from heavy metals exposure has been reported,[45] and some environmental toxins such as rotenone have also been reported to cause α-synuclein aggregation. In our results, abnormal accumulation and phosphorylation of α-synuclein protein were verified in the SNpc of rats after CS_2 exposure. The strong positive correlation between α-synuclein deposition and SNs loss has long been reported.[46,47] In our results, ELN484228, an α-synuclein protein inhibitor, protected against cell death while inhibiting programmed necrosis signaling pathway expression, which emphasizes the role of α-synuclein as a major pathological protein of cell death. The coexistence of α-synuclein aggregation and necrosis signaling activation implies that α-synuclein may directly activate necrosis signaling, and most valuable is that this link was further validated *in vivo*, *in vitro*, and in silico level. These findings may contribute to the knowledge of necroptosis and α-synuclein in the death of dopaminergic neurons induced by CS_2 and other environmental toxicants.

Table 1. Interaction specific of αS and necrosome

	RIP: 4itj		RIP3: 7mx3		MLKL: 4mwi		RIP3-MLKL: 7mon	
	ΔiG kcal/M	ΔiG p-value	ΔiG kcal/M	ΔiG p-value	ΔiG kcal/M	ΔiG p-value	ΔiG kcal/M	ΔiG p-value
αS: 6i42	−3.8		−14.1		−8.4		−19.3	
αS: 3q25	5.5		−12.8		/		−13.7	
αS: 1xq8	−8.6		−15.4	0.074	/		−32.8	0.113

Note: ΔiG indicates the solvation-free energy gain upon formation of the interface, in kcal/M. Negative ΔiG corresponds to hydrophobic interfaces or positive protein affinity. The p-value is a measure of interface specificity, showing how surprising, in energy terms, the interface is. $p < 0.5$ indicates interfaces with surprising (higher than would-be-average for given structures) hydrophobicity, implying that the interface surface can be interaction specific.

In conclusion, CS_2 induced aberrant α-synuclein accumulation to trigger the necroptosis of dopaminergic neurons in rat midbrain, which finally results in the parkinsonism-like behavior of rats. We revealed the potential interaction between necroptosis and α-synuclein and providing insight into the development of parkinsonism. Further investigation into this relationship may contribute to the development of effective treatments and strategies for preventing or delaying the onset of these debilitating conditions.

Limitations of the study

Our animal experiments were performed with male rats, gender or sex factors may have an impact. Cellular intervention experiments through SH-SY5Y cell line may not fully mimic the complexity of the human nervous system. We used intervening drugs to intervene the expression of α-synuclein and RIPK3 proteins, and the conclusions obtained may differ from those of the genetic intervention.

STAR★METHODS

Detailed methods are provided in the online version of this paper and include the following:

- KEY RESOURCES TABLE
- RESOURCE AVAILABILITY
  - Lead contact
  - Materials availability
  - Data and code availability
- EXPERIMENTAL MODEL AND STUDY PARTICIPANT DETAILS
  - Cell lines
  - Rat
- METHOD DETAILS
  - Animal exposure and behavioral testing
  - Immunofluorescence and In Situ Cell Death Detection
  - Immunoblotting and co-immunoprecipitation (Co-IP)
  - Transmission electron microscopy
  - In the vitro reaction system
  - Cell culture
- QUANTIFICATION AND STATISTICAL ANALYSIS

SUPPLEMENTAL INFORMATION

Supplemental information can be found online at https://doi.org/10.1016/j.isci.2023.107787.

ACKNOWLEDGMENTS

We thank the Experimental Platform of School of Public Health, Shandong University, for supporting the experimental techniques.

Funding: Fuyong Song was funded by the "National Natural Science Foundation of China" (No. 82173552), Yao Bai was funded by a grant (2017YFC1601103) from the Ministry of Science and Technology of the People's Republic of China.

AUTHOR CONTRIBUTIONS

F. S. and Y. B. directed the study. F.S. and Z.L. conceptualized the study, Z.L. performed experiments. K.K., S.S., S.W., X.L., H.Y., Z.H., Y.Y., Z.L., and Y.S. provided experimental assistance. Z.L. wrote the original manuscript writing and edited the figures. F.S., Y.B., and Z.L. contributed to editing and reviewing. F.S. and Y.B. raised funding for the study.

DECLARATION OF INTERESTS

The authors declare no competing interests.

INCLUSION AND DIVERSITY

We support inclusive, diverse, and equitable conduct of research.

Received: March 17, 2023
Revised: June 27, 2023
Accepted: August 28, 2023
Published: August 30, 2023

REFERENCES

1. de Rijk, M.C., Rocca, W.A., Anderson, D.W., Melcon, M.O., Breteler, M.M., and Maraganore, D.M. (1997). A population perspective on diagnostic criteria for Parkinson's disease. Neurology *48*, 1277–1281. https://doi.org/10.1212/wnl.48.5.1277.
2. Bloem, B.R., Okun, M.S., and Klein, C. (2021). Parkinson's disease. Lancet *397*, 2284–2303. https://doi.org/10.1016/S0140-6736(21)00218-X.
3. Dorsey, E.R., Sherer, T., Okun, M.S., and Bloem, B.R. (2018). The Emerging Evidence of the Parkinson Pandemic. J. Parkinsons Dis. *8*. S3–s8. https://doi.org/10.3233/jpd-181474.
4. Langston, J.W., Langston, E.B., and Irwin, I. (1984). MPTP-induced parkinsonism in human and non-human primates–clinical and experimental aspects. Acta Neurol. Scand. Suppl. *100*, 49–54.
5. Chand, P., and Litvan, I. (2007). Parkinson's Disease. In Encyclopedia of Gerontology, Second Edition, J.E. Birren, ed. (Elsevier), pp. 322–333. https://doi.org/10.1016/B0-12-370870-2/00146-3.
6. Jorgenson, J.L. (2001). Aldrin and dieldrin: a review of research on their production, environ mental deposition and fate, bioaccumulation, toxicology, and epidemiol ogy in the United States. Environ. Health Perspect. *109*, 113–139. https://doi.org/10.1289/ehp.01109s1113.
7. Jollow, D.J., Bruckner, J.V., McMillan, D.C., Fisher, J.W., Hoel, D.G., and Mohr, L.C. (2009). Trichloroethylene risk assessment: a review and commentary. Crit. Rev. Toxicol. *39*, 782–797. https://doi.org/10.3109/10408440903222177.
8. Delpech, A. (1856). Note sur les accidents que dévelope, chez les ouvriers en caoutchouc, l'inhalation du sulfure de carbone en vapeur. Académie Impériale de Médecine *21*, 350.
9. Spencer, P. (1980). Experimental and Clinical Neurotoxicology (Williams & Wilkins).
10. Rosenberg, N., and Denver. (1995). Occupational and Environmental Neurology (Butterworth-Heinemann).
11. Albin, R.L., and Roger, L.J.N.C. (2000). Basal ganglia neurotoxins. Neurol. Clin. *18*, 665–680.
12. Moretto, A., and Colosio, C. (2011). Biochemical and toxicological evidence of neurological effects of pesticides: the example of Parkinson's disease. Neurotoxicology *32*, 383–391. https://doi.org/10.1016/j.neuro.2011.03.004.
13. Brown, T.P., Rumsby, P.C., Capleton, A.C., Rushton, L., and Levy, L.S. (2006). Pesticides and Parkinson's disease–is there a link? Environ. Health Perspect. *114*, 156–164. https://doi.org/10.1289/ehp.8095.
14. Zhou, Y., Shie, F.S., Piccardo, P., Montine, T.J., and Zhang, J. (2004). Proteasomal inhibition induced by manganese ethylene-bis-dithiocarbamate: relevance to Parkinson's disease. Neuroscience *128*, 281–291. https://doi.org/10.1016/j.neuroscience.2004.06.048.
15. Fitzmaurice, A.G., Rhodes, S.L., Cockburn, M., Ritz, B., and Bronstein, J.M. (2014). Aldehyde dehydrogenase variation enhances effect of pesticides associated with Parkinson disease. Neurology *82*, 419–426. https://doi.org/10.1212/wnl.0000000000000083.
16. Yuan, J., Amin, P., and Ofengeim, D. (2019). Necroptosis and RIPK1-mediated neuroinflammation in CNS diseases. Nat. Rev. Neurosci. *20*, 19–33. https://doi.org/10.1038/s41583-018-0093-1.
17. Christofferson, D.E., Li, Y., Hitomi, J., Zhou, W., Upperman, C., Zhu, H., Gerber, S.A., Gygi, S., and Yuan, J. (2012). A novel role for RIP1 kinase in mediating TNFα production. Cell Death Dis. *3*, e320. https://doi.org/10.1038/cddis.2012.64.
18. Degterev, A., Hitomi, J., Germscheid, M., Ch'en, I.L., Korkina, O., Teng, X., Abbott, D., Cuny, G.D., Yuan, C., Wagner, G., et al. (2008). Identification of RIP1 kinase as a specific cellular target of necrostatins. Nat. Chem. Biol. *4*, 313–321. https://doi.org/10.1038/nchembio.83.
19. Lin, Q.S., Chen, P., Wang, W.X., Lin, C.C., Zhou, Y., Yu, L.H., Lin, Y.X., Xu, Y.F., and Kang, D.Z. (2020). RIP1/RIP3/MLKL mediates dopaminergic neuron necroptosis in a mouse model of Parkinson disease. Lab. Invest. *100*, 503–511. https://doi.org/10.1038/s41374-019-0319-5.
20. Schlossmacher, M.G., Frosch, M.P., Gai, W.P., Medina, M., Sharma, N., Forno, L., Ochiishi, T., Shimura, H., Sharon, R., Hattori, N., et al. (2002). Parkin localizes to the Lewy bodies of Parkinson disease and dementia with Lewy bodies. Am. J. Pathol. *160*, 1655–1667. https://doi.org/10.1016/s0002-9440(10)61113-3.
21. Huang, H.J., Wang, H.T., Yeh, T.Y., Lin, B.W., Shiao, Y.J., Lo, Y.L., and Lin, A.M.Y. (2021). Neuroprotective effect of selumetinib on acrolein-induced neurotoxicity. Sci. Rep. *11*, 12497. https://doi.org/10.1038/s41598-021-91507-6.
22. Liu, Y.L., Hsu, C.C., Huang, H.J., Chang, C.J., Sun, S.H., and Lin, A.M.Y. (2020). Gallic Acid Attenuated LPS-Induced Neuroinflammation: Protein Aggregation and Necroptosis. Mol. Neurobiol. *57*, 96–104. https://doi.org/10.1007/s12035-019-01759-7.
23. Aaserud, O., Hommeren, O.J., Tvedt, B., Nakstad, P., Mowé, G., Efskind, J., Russell, D., Jörgensen, E.B., Nyberg-Hansen, R., Rootwelt, K., et al. (1990). Carbon disulfide exposure and neurotoxic sequelae among viscose rayon workers. Am. J. Ind. Med. *18*, 25–37. https://doi.org/10.1002/ajim.4700180104.
24. Aaserud, O., Russell, D., Nyberg-Hansen, R., Rootwelt, K., Jörgensen, E.B., Nakstad, P., Hommeren, O.J., Tvedt, B., and Gjerstad, L. (1992). Regional cerebral blood flow after long-term exposure to carbon disulfide. Acta Neurol. Scand. *85*, 266–271. https://doi.org/10.1111/j.1600-0404.1992.tb04042.x.
25. Dietzmann, K., and Laass, W. (1977). Histological and histochemical studies on the rat brain under conditions of carbon disulfide intoxication. Exp. Pathol. *13*, 320–327. https://doi.org/10.1016/s0014-4908(77)80019-7.
26. Beauchamp, R.O., Jr., Bus, J.S., Popp, J.A., Boreiko, C.J., Goldberg, L., and Goldberg. (1983). A critical review of the literature on carbon disulfide toxicity. Crit. Rev. Toxicol. *11*, 169–278. https://doi.org/10.3109/10408448309128255.
27. Graham, D.G., Amarnath, V., Valentine, W.M., Pyle, S.J., and Anthony, D.C. (1995). Pathogenetic studies of hexane and carbon disulfide neurotoxicity. Crit. Rev. Toxicol. *25*, 91–112. https://doi.org/10.3109/10408449509021609.
28. Wang, S., Irving, G., Jiang, L., Wang, H., Li, M., Wang, X., Han, W., Xu, Y., Yang, Y., Zeng, T., et al. (2017). Oxidative Stress Mediated Hippocampal Neuron Apoptosis Participated in Carbon Disulfide-Induced Rats Cognitive Dysfunction. Neurochem. Res. *42*, 583–594. https://doi.org/10.1007/s11064-016-2113-8.
29. Irving, G., Wang, S., Wang, H., Guo, Y., Jiang, L., Zhao, X., and Xie, K. (2015). Effects of carbon disulfide on the learning ability of rats and its underlying mechanisms. J. Shandong Univ. Health Sci. *53*, 82–86.
30. Gutsev, G.L., Bartlett, R.J., and Compton, R.N. (1998). Electron affinities of CO2. J. Chem. Phys. *108*, 6756–6762. https://doi.org/10.1063/1.476091.
31. McKee, R.W. (1941). Solubility of carbon disulfide vapor in body fluids and tissues. Ind. Hyg. Toxicol *23*, 484–489.
32. Valentine, W.M., Amarnath, V., Amarnath, K., Rimmele, F., and Graham, D.G. (1995). Carbon disulfide mediated protein cross-linking by N,N-diethyldithiocarbamate. Chem. Res. Toxicol. *8*, 96–102. https://doi.org/10.1021/tx00043a013.
33. DeMartino, A.W., Zigler, D.F., Fukuto, J.M., and Ford, P.C. (2017). Carbon disulfide. Just toxic or also bioregulatory and/or

therapeutic? Chem. Soc. Rev. *46*, 21–39. https://doi.org/10.1039/c6cs00585c.

34. Richter, F., Hamann, M., and Richter, A. (2007). Chronic rotenone treatment induces behavioral effects but no pathological signs of parkinsonism in mice. J. Neurosci. Res. *85*, 681–691. https://doi.org/10.1002/jnr.21159.
35. Lewey, F., Alpers, B., Bellet, S., Creskoff, A., Drabkin, D., Ehrich, W., Frank, J., Jonas, L., McDonald, R., Montgomery, E., and Reinhold, J. (1941). Experimental chronic carbon disulfide poisoning in dogs: a clinical, biochemical and pathological study. J. Ind. Hyg. and Toxicol. *23*, 415–436.
36. Godderis, L., Braeckman, L., Vanhoorne, M., and Viaene, M. (2006). Neurobehavioral and clinical effects in workers exposed to CS2. Int. J. Hyg Environ. Health *209*, 139–150. https://doi.org/10.1016/j.ijheh.2005.09.005.
37. Hageman, G., van der Hoek, J., van Hout, M., van der Laan, G., Steur, E.J., de Bruin, W., and Herholz, K. (1999). Parkinsonism, pyramidal signs, polyneuropathy, and cognitive decline after long-term occupational solvent exposure. J. Neurol. *246*, 198–206. https://doi.org/10.1007/s004150050334.
38. Chi, H., Chang, H.Y., and Sang, T.K. (2018). Neuronal Cell Death Mechanisms in Major Neurodegenerative Diseases. Int. J. Mol. Sci. *19*, 3082. https://doi.org/10.3390/ijms19103082.
39. Ross, G.W., Petrovitch, H., Abbott, R.D., Nelson, J., Markesbery, W., Davis, D., Hardman, J., Launer, L., Masaki, K., Tanner, C.M., and White, L.R. (2004). Parkinsonian signs and substantia nigra neuron density in decendents elders without PD. Ann. Neurol. *56*, 532–539. https://doi.org/10.1002/ana.20226.
40. Weinlich, R., Oberst, A., Beere, H.M., and Green, D.R. (2017). Necroptosis in development, inflammation and disease. Nat. Rev. Mol. Cell Biol. *18*, 127–136. https://doi.org/10.1038/nrm.2016.149.
41. Wu, X.N., Yang, Z.H., Wang, X.K., Zhang, Y., Wan, H., Song, Y., Chen, X., Shao, J., and Han, J. (2014). Distinct roles of RIP1-RIP3 hetero- and RIP3-RIP3 homo-interaction in mediating necroptosis. Cell Death Differ. *21*, 1709–1720. https://doi.org/10.1038/cdd.2014.77.
42. Iannielli, A., Bido, S., Folladori, L., Segnali, A., Cancellieri, C., Maresca, A., Massimino, L., Rubio, A., Morabito, G., Caporali, L., et al. (2018). Pharmacological Inhibition of Necroptosis Protects from Dopaminergic Neuronal Cell Death in Parkinson's Disease Models. Cell Rep. *22*, 2066–2079. https://doi.org/10.1016/j.celrep.2018.01.089.
43. Spillantini, M.G., Schmidt, M.L., Lee, V.M., Trojanowski, J.Q., Jakes, R., and Goedert, M. (1997). Alpha-synuclein in Lewy bodies. Nature *388*, 839–840. https://doi.org/10.1038/42166.
44. Balestrino, R., and Schapira, A.H.V. (2020). Parkinson disease. Eur. J. Neurol. *27*, 27–42. https://doi.org/10.1111/ene.14108.
45. Uversky, V.N., Li, J., and Fink, A.L. (2001). Metal-triggered structural transformations, aggregation, and fibrillation of human alpha-synuclein. A possible molecular NK between Parkinson's disease and heavy metal exposure. J. Biol. Chem. *276*, 44284–44296. https://doi.org/10.1074/jbc.M105343200.
46. Dijkstra, A.A., Voorn, P., Berendse, H.W., Groenewegen, H.J., Netherlands Brain Bank, Rozemuller, A.J.M., and van de Berg, W.D.J. (2014). Stage-dependent nigral neuronal loss in incidental Lewy body and Parkinson's disease. Mov. Disord. *29*, 1244–1251. https://doi.org/10.1002/mds.25952.
47. Braak, H., Del Tredici, K., Rüb, U., de Vos, R.A.I., Jansen Steur, E.N.H., and Braak, E. (2003). Staging of brain pathology related to sporadic Parkinson's disease. Neurobiol. Aging *24*, 197–211. https://doi.org/10.1016/s0197-4580(02)00065-9.
48. Liu, Z.W., Zhuang, Z.C., Chen, R., Wang, X.R., Zhang, H.L., Li, S.H., Wang, Z.Y., and Wen, H.L. (2019). Enterovirus 71 VP1 Protein Regulates Viral Replication in SH-SY5Y Cells via the mTOR Autophagy Signaling Pathway. Viruses *12*, 11. https://doi.org/10.3390/v12010011.

STAR★METHODS

KEY RESOURCES TABLE

REAGENT or RESOURCE	SOURCE	IDENTIFIER
Antibodies		
Mouse monoclonal Anti-Tyrosine Hydroxylase	Sigma-Aldrich	Cat#MAB318; RRID: AB_2201528
Rabbit monoclonal Anti- Synaptophysin	Cell Signaling Technology	Cat# 36406; RRID: AB_2799098
Rabbit monoclonal Anti-Phospho-α-Synuclein (Ser129)	Cell Signaling Technology	Cat# 23706; RRID: AB_2798868
Rabbit monoclonal Anti-alpha -Synuclein	Cell Signaling Technology	Cat# 4179; RRID: AB_1904156
Rabbit monoclonal Anti-RIP	Cell Signaling Technology	Cat# 3493; RRID: AB_2305314
Rabbit monoclonal Anti- Phospho-RIP (Ser166)	Cell Signaling Technology	Cat# 53286; RRID: AB_2925183
Rabbit polyclonal Anti-RIP3	Abcam	Cat#ab62344; RRID: AB_956268
Rabbit polyclonal Anti-Phospho-RIP3 (Ser227)	Cell Signaling Technology	Cat# 93654; RRID: AB_2800206
Rabbit polyclonal Anti-MLKL	Abcam	Cat#ab172868; RRID: AB_2737025
Rabbit monoclonal Anti-MLKL (phospho S345)	Abcam	Cat#ab196436; RRID: AB_2687465
Mouse monoclonal Anti-β-Actin	Sigma-Aldrich	Cat#A5441; RRID: AB_476744
Chemicals, peptides, and recombinant proteins		
Carbon disulfide	sinopharm	Cat#10006318
RA	Sigma-Aldrich	Cat#102436622
DMSO	Klontech	Cat#C2H6S0
GSK872	MCE	Cat#HY-101872
ELN484228	MCE	Cat#HY-115038
Critical commercial assays		
Pierce Co-Immunoprecipitation (Co-IP) Kit	Thermo Fisher	Cat#26149
In Situ Cell Death Detection Kit	Roche	Cat#11684795910
Experimental models: Cell lines		
SH-SY5Y cells	ATCC	CRL-2266
Experimental models: Organisms/strains		
Rat: Wistar, Wild type	Jinan Pengyue	No.370726201100653321
Software and algorithms		
ImageJ	Fiji software	https://imagej.nih.gov/ij/
GraphPad Prism v.8.0	GraphPad Software	https://www.graphpad.com/
Origin 2023b	Origin Software	https://www.originlab.com/
SPSS 18	IBM SPSS Software	https://www.ibm.com/

RESOURCE AVAILABILITY

Lead contact

Further information and requests for resources and reagents should be directed to and will be fulfilled by the lead contact, Fuyong Song Fysong3707@sdu.edu.cn.

Materials availability

This study did not generate new unique reagents.

Data and code availability

- Data reported in this paper will be shared by the lead contact upon request.
- This paper does not report original code.
- Any additional information required to reanalyze the data reported in this paper is available from the lead contact upon request.

EXPERIMENTAL MODEL AND STUDY PARTICIPANT DETAILS

Cell lines

SH-SY5Y cell line are a generous gift form Pr Zi-wei Liu.[48] Specific experimental steps are described in the method details section.

Rat

This study was conducted with 7- to 9-week-old (about 300g body weight) Male Wistar rats. Rats were maintained under pathogen-free conditions and all procedures and experiments were carried out according to institutional guidelines for the Animal Care and Use Committee at Shandong University (China). Specific experimental steps are described in the method details section.

METHOD DETAILS

Animal exposure and behavioral testing

Male WISTAR rats with 300g body weight were exposed to CS_2 for 8 weeks by intragastric administration at doses of 0mg/kg, 300mg/kg, and 600mg/kg. Before animals were sacrificed, the behavioral analysis includes the incidence of resting tremor, latency to fall of rotarod, and gait score proceeding every week. Incidence of resting tremor. To capture the resting tremor which is typical in PD, rats were placed in an open field, quiet environment and were observed for 10 minutes. Rats who showed resting tremor was recorded and the incidence of resting tremor was counted. Typical videos of resting tremors were collected. Latency to fall of rotarod. To measure motor ability, rats were trained on the rotarod at 5 RPM for 300 seconds, one day before testing. Then rats were placed on a rotarod which accelerated from 5 to 40 RPM over 300 seconds. Each rat was tested three times with each trial separated by a minimum of 20 minutes. The average latency to fall of the rotarod was counted. Gait score. To measure gait disorder, rats were placed in an open field, following 3 minutes of observation, a gait score from 1 to 4 (1= normal gait; 2= slightly abnormal gait; 3= markedly ataxia, swaying, stumbling, splaying hindlimbs; 4= severely abnormal gait like flat foot, crawling, unable to support weight) was assigned. Typical images of gait disorders were collected.

Immunofluorescence and In Situ Cell Death Detection

The rat was anesthetized with chloral hydrate, and perfused transcardially with PBS 100ml, followed by 300ml of 4% paraformaldehyde for fixation. The brain was dissected rapidly and fixed with 4% paraformaldehyde overnight at 4°C, dehydrated with 30% sucrose for over 24 hours at 4°C, and embedded with OCT. Then, the brain was sectioned at 40μm per slice using a freezing microtome (Thermo, micron HM 525), and cryopreserved in 0.02% sodium azide at 4°C. For immunostaining, slices were permeabilized and blocked with 0.3% Triton X-100, 5% Goat Serum, 5% BSA, and 0.1M glycine in PBS for 1 h at room temperature. Then, slices were incubated with primary antibodies (TH, 1:300, Sigma, MAB318; SYN, 1:300, CST 36406; p-MLKL(S345), 1:300, Abcam ab196436; p-α-synuclein (S129), 1:300, CST 23706) in PBS containing 1% BSA, 0.3% TritonX-100 overnight at 4°C. After being washed with PBS, slices were incubated with Secondary antibodies (Alexa Fluor 488 Goat anti-mouse IgG, 1:1000, Thermo, A11004; Alexa Fluor 568 Goat anti-Rabbit IgG, 1:1000, Thermo, A11011) in PBS containing 1% BSA for 2h at room temperature and dark environment. After being washed with PBS, nuclei were stained with DAPI in Prolong Gold anti-fade reagent (Thermo, P36930). For *In Situ* Cell Death staining, slices were strictly processed following *In Situ* Cell Death Detection Kit (Roche 11684795910) instructions. After staining, slides were visualized and captured using a confocal microscope (ZEISS, Axio Vert.A1). No nonspecific staining was observed with the secondary antibody alone. All comparative stains from control and exposed rats were acquired using identical laser and microscope settings.

Immunoblotting and co-immunoprecipitation (Co-IP)

The rat was anesthetized with chloral hydrate. Perfused transcardially with PBS 100ml, brain tissues were dissected rapidly and placed in liquid nitrogen, then store at -80. For Immunoblotting, the brain was homogenized and lysed with ice-cold RIPA buffer (50mM Tris, 150mM NaCl, 0.5% Sodium deoxycholate, 0.1% SDS, 1% Triton x-100) containing protease and phosphatase inhibitors (Thermo 78441) and centrifuged at 12,000 RPM for 20 minutes at 4°C. For co-immunoprecipitation, brain tissues were processed following Pierce Co-Immunoprecipitation (Co-IP) Kit (Thermo 26149) instructions strictly, and anti-α-synuclein antibodies (CST, 4179) were used as bait protein. Anti-rabbit IgG (zsbio, ZB-2301) was used as control. Protein concentration was determined by a BCA (bicinchoninicacid) assay (Thermo 23225) and 40 mg of total protein was separated by SDS-PAGE and transferred to transfer membranes (Millipore IPVH00010). Membranes were blocked using 5% milk in TBST (50 mM Tris, 150 mM NaCl, 0.1% Tween 20, pH 7.4) for 1 hour at room temperature and incubated with primary antibodies (TH, sigma, MAB318; SYN, CST, 36406; RIP1, CST, 3493; p-RIP1(S166), CST, 53286; RIP3, abcam, ab62344; p-RIP3(S227), CST, 93654; MLKL, abcam, ab172868; p-MLKL(S345), abcam, ab196436; α-synuclein, CST, 4179; p-α-synuclein (S129), CST, 23706) overnight at 4°C. After being washed with TBST, Membranes were incubated with appropriate HRP-conjugated secondary antibodies (Goat anti-rabbit IgG, HRP-Linked, zsbio, ZB-2301; Goat anti-mouse IgG, HRP-Linked, zsbio, ZB-2305) for 1 hour at room temperature. Followed by washing with TBST extensively, target proteins were probed and captured using a Chemiluminescence imager (GE, Amersham Imager 600). Images were quantified with FIJI (win-64). All images were analyzed from at least two technical replicates.

Transmission electron microscopy

Rat brain tissues containing SNpc region were fixed with 2.5% glutaraldehyde (Aladdin, G105907) for 2 h at RT (room temperature), washed with 0.1 M phosphate buffer (KH2PO4, Na2HPO4, pH 7.4), post-fixed in 1% osmium tetroxide for 2 h at RT, washed again. The brain tissues

were dehydrated with 50%, 70%, and 90% ethanol, a mixture of 45% ethanol and 45% acetone, 90% acetone successively for 20 min in each solution at 4°C, and 100% acetone for 20 min at RT. Then, brain tissues were embedded in epoxy resin and solidified. Then, serial ultrathin sections (70 nm) of SNpc regions were collected and stained. The synaptic junction and mitochondria of SNpc neurons were observed with transmission electron microscopy (JEM-1230). The images were captured by a CCD camera (Olympus) and counted using FIJI (win-64) software.

In the vitro reaction system

Brain protein supernatant was obtained from the control group for Immunoblotting, add 500ul of supernatant to two EP tubes respectively, add 30ul of carbon disulfide or water to two EP tubes respectively. The EP tubes were then sealed and placed at 37°C overnight. Following, the supernatant was added non-reducing lording buffer and processing Immunoblotting.

Cell culture

SH-SY5Y cells were grown in DMEM medium (cytiva-SH30243.01) supplemented with 10% fetal bovine serum (Gibco, 12484028), 1%Penicillin-streptomycin (Macgene-CC004) with 5% CO_2 at 37°C. Differentiation to a dopaminergic neuron was achieved using 8uM RA (sigma-102436622) for 3 days. Then, CS_2 (sinopharm-10006318) or vehicle (DMSO, Klontech, C2H6S0) exposure was proceeding, GSK872 (MCE, HY-101872) or ELN484228 (MCE, HY-115038) was pre-administration 3 hours. After two day's exposure, the morphology of cells was observed by an optical microscope (JiangNan, XD-202), captured by a CMOS (complementary metal-oxide-semiconductor) camera (ISH500), and counted using Fiji (win-64) software. Then, cells were carried out with immunoblotting assays.

QUANTIFICATION AND STATISTICAL ANALYSIS

All data are shown as mean with SEM. Equal variances were tested using the Brown-Forsythe test. When variances were normality or homogeneity, *t*-test, One-Way, or Two Way ANOVA was used. For non-parametric data, the Mann-Whitney U test or Kruskal-Wallis test was used. Statistical comparison was performed with SPSS software, graphs generation was performed with GraphPad Prism 7 software and Origin software. When $p < 0.05$, we considered it statistically significant. The Figure was partly generated using Servier Medical Art, provided by Servier, licensed under a Creative Commons Attribution 3.0 unported license. And partly drawn using Figdraw (ID:AOYPIdea47).